J. Biochem. 124, 602-608 (1998)

Fluorescence Energy Transfer of Complexes of Skeletal Muscle Troponin C and Melittin Derivatives

Hiroki Sano,*,[1] Sho Takahashi,† and Takayoshi Iio*

*Department of Physics, Faculty of Science, Nagoya University, Chikusa-ku, Nagoya, Aichi 464-8602; and †Institute for Chemical Research, Kyoto University, Gokasho, Uji, Kyoto 611-0011

Received for publication, April 22, 1998

We studied Ca^{2+}-dependent structural change of rabbit skeletal troponin C (TnC)-melittin (ME) complex as a model of TnC-troponin I complex. In previous study, we found that the distance between Met-25 and Cys-98 of TnC in TnC-ME complex increased upon binding of Ca^{2+} to TnC [H. Sano and T. Iio (1995) *J. Biochem.* 118, 996-1000]. In this study, we used a fluorescence energy transfer method. As a fluorescent donor, we used the tryptophan residue in four melittin derivatives, in which residue 2, 5, 8, or 13 was replaced with tryptophan. As acceptor, we used dansylaziridine (DANZ) bound to Met-25 of TnC, or *N*-iodoacetyl-*N'*-(5-sulfo-1-naphthyl)ethylenediamine (1,5-I-AEDANS) bound to Cys-98 of TnC. For all TnC^{DANZ}-ME complexes, the donor-acceptor distance (11.9-17.7 Å) did not remarkably depend on Mg^{2+} or Ca^{2+} binding of TnC or on the position of tryptophan in ME derivatives. The same results were obtained for TnC^{AEDANS}-ME complexes in the absence of Ca^{2+} (distance 15.2-21.7 Å). But in the presence of Ca^{2+}, tryptophan residues in the central region of ME were near to Cys-98 of TnC (distance much less than 10.4 Å). Based on these results, we conclude that ME is enfolded by the N- and C-lobes of TnC, and the ME rod is almost perpendicular to a line connecting Met-25 and Cys-98 of TnC. The position of the ME rod shifts upon binding of Ca^{2+} to TnC.

Key words: calcium ion, fluorescence energy transfer, melittin, structural change, troponin C.

Skeletal muscle troponin C (TnC) is a Ca^{2+}-binding protein (*1*). It is a subunit of the troponin molecule, which, with tropomyosin, regulates Ca^{2+}-dependently the actomyosin ATPase and the force generation of skeletal muscle (see reviews in Refs. *1-4*). TnC assumes a dumbbell shape, consisting of two lobes which are connected by a central helix (*5, 6*). It contains four Ca^{2+}-binding sites (*5, 6*). Sites I and II are low affinity Ca^{2+}-binding sites in the N-terminal lobe, and sites III and IV are high affinity Ca^{2+}/Mg^{2+}-binding sites in the C-terminal lobe (*7-10*). Calmodulin, another Ca^{2+}-binding protein, is a close homolog of TnC (*11*) and assumes the same type of the three-dimensional structure (*12*).

TnC undergoes structural change upon Ca^{2+} binding, and this structural change has been considered to be essential for the biological role of TnC (*13*). For instance, Herzberg *et al.* (*14*) proposed that Ca^{2+} binding to the low affinity sites induces a structural transition of the N-terminal domain (regulatory domain) of TnC to produce a similar structure to that of the C-terminal domain, which binds Ca^{2+} or Mg^{2+} under physiological conditions, and that the structural transition is essential for the biological role of TnC. Houdusse *et al.* (*15*) determined crystal structure of 4 Ca^{2+}-bound TnC and confirmed the proposal of Herzberg *et al.* The experiments of Grabarek *et al.* (*16*) and Fujimori *et al.* (*17*) revealed also that restrictions of the structural transition of the N-terminal domain reduced the biological function of TnC.

It is well known that some Ca^{2+}-binding proteins interact Ca^{2+}-dependently with short basic amphipathic peptides (*18, 19*). These peptides have common structural features of notable clusters of basic amino acid residues in close conjunction with hydrophobic amino acid sequences. One such peptide is honey bee venom melittin (ME), a 26-residue peptide (*20*). The complexes of melittin and Ca^{2+}-binding proteins have been regarded as useful models of protein-protein interactions. For example, the Ca^{2+}-dependent interaction between melittin and calmodulin has been extensively studied (*18, 21*).

In the troponin molecule, TnC binds to the residues 1-47 and 101-113 of troponin I (*4, 13, 22-26*). In the binary complex of troponin I and TnC, Wang and Cheung (*27*) reported that the distance between Met-25 and Cys-98 of TnC increased upon binding of Ca^{2+} to sites I and II. In a previous study, based on a similarity between amino acid sequences, we used melittin as a model of the TnC-binding troponin I peptide of residues 101-113. We found that the distance between Met-25 and Cys-98 of TnC in TnC-ME complex increased upon binding of Ca^{2+} to TnC (*28*). In this paper, we report a study of the Ca^{2+}-dependent structural

[1] To whom correspondence should be addressed. E-mail: zetha@white.plala.or.jp

Abbreviations: DANZ, dansylaziridine; EGTA, ethylene glycol bis-(β-aminoethyl ether)-*N,N,N',N'*-tetraacetic acid; 1,5-I-AEDANS, *N*-iodoacetyl-*N'*-(5-sulfo-1-naphthyl)ethylenediamine; ME, bee venom melittin; TnC, rabbit skeletal muscle troponin C.

change of TnC-melittin complex by a fluorescence energy transfer method using four melittin derivatives, in which residue 2, 5, 8, or 13 of melittin was replaced with tryptophan.

MATERIALS AND METHODS

Troponin-tropomyosin complex was extracted from rabbit skeletal muscle (*29*), and troponin was separated from tropomyosin by the isoelectric precipitation method (*29*). Three components of troponin were separated by ion exchange chromatography as reported in Ref. *30*. The concentration of TnC was determined by spectrophotometry using A_{277} (1 mg/ml) = 0.23 (*31*) and a molecular weight of 18,000 (*8*).

Bee venom melittin was purchased from Sigma Chemical and further purified by the method of Maulet *et al.* (*32*) with modification. Melittin was dissolved in a solution containing 4 M urea and 0.05 M ammonium acetate, pH 4.75, and applied to a column of CM-Sephadex C25. ME was eluted with a gradient of 0.15-0.3 M KCl in the same buffer. The buffer system of the solution was replaced with a solution containing 0.1 M KCl, 4 mM EGTA, and 20 mM Tris-HCl, pH 7.5, by gel chromatography on Sephadex G-50F. Melittin concentration was determined using a molar extinction coefficient of 5,470 $M^{-1} \cdot cm^{-1}$ at 280 nm (*33*).

Melittin derivatives were synthesized by a solid-phase method with a fluorenyl-methyloxycarbonyl group for temporary protection of the α-amino group of component amino acids. The synthesis was carried out on a model 431A peptide synthesizer of Applied Biosystems with a FastMoc protocol supplied by the manufacturer at 0.1 mmol peptide quantity. The peptides were purified by the same method as used for native melittin. We synthesized four melittin derivatives, I2W/W19L, V5W/W19L, V8W/W19L, and L13W/W19L, and their amino acid sequences are shown in Fig. 1. Since the experimentally determined molar extinction coefficients of the synthetic peptides were the same as that of the native melittin, the concentrations of the synthesized melittin derivatives were determined using the molar extinction coefficient of 5,470 $M^{-1} \cdot cm^{-1}$ at 280 nm.

In the fluorescence energy transfer experiment, dansylaziridine (DANZ) and *N*-iodoacetyl-*N'*-(5-sulfo-1-naphthyl)ethylenediamine (1,5-I-AEDANS) were used as acceptors. DANZ and 1,5-I-AEDANS were purchased from Merck Chemical and Sigma Chemical, respectively. Modification of Met-25 of TnC with DANZ was performed by the method of Johnson *et al.* (*34*). The concentration of DANZ bound to TnC was determined using $A_{350} = 3{,}980\ M^{-1} \cdot cm^{-1}$ (*34*). Modification of Cys-98 of TnC with 1,5-I-AEDANS was performed by the method of Grabarek *et al.* (*35*). The concentration of AEDANS bound to TnC was determined using $A_{337} = 6{,}000\ M^{-1} \cdot cm^{-1}$ (*36*). The protein concentration of the fluorescent probe-TnC complex was determined according to Lowry *et al.* (*37*). The molar ratio of the fluorescent probe to the protein was 80.6 ± 1.8% in TnC^{DANZ} and 49.8 ± 1.0% in TnC^{AEDANS}.

Absorption spectra were measured with a Hitachi U-3300 spectrophotometer. Fluorescence spectra were measured with a Hitachi F-4500 fluorescence spectrophotometer.

Transfer efficiency of resonance energy from donor to acceptor was determined by measuring the degree of quenching of steady-state donor fluorescence intensity (*38, 39*). The transfer efficiency E was calculated from the following equation:

$$E = 1 - (F_{DA}/F_D) \quad (1)$$

where F_D is the emission intensity of the donor in TnC-ME complex or TnC-ME derivative complexes, and F_{DA} is the corrected emission intensity of the donor in TnC^{DANZ}-ME, TnC^{DANZ}-ME derivatives, TnC^{AEDANS}-ME, or TnC^{AEDANS}-ME derivatives. The emission intensity of the donor in the fluorescence-labeled TnC-ME was corrected for nonstoichiometric labeling of the acceptor and for the absorption of the emission light by the acceptor.

The Förster critical transfer distance R_0 (Å) (*40*) was calculated from

$$R_0^6 = (8.79 \times 10^{-5}) n^{-4} Q_D \kappa^2 J \quad (2)$$

where n is the refractive index of the solvent and was taken as 1.40; Q_D is the donor quantum yield, which was determined using quinine sulfate as a standard (*41*); κ^2 is the orientation factor; and J is the spectral overlap integral calculated from the fluorescence spectrum $F_D(\lambda)$ of the donor and absorption spectrum $\varepsilon_A(\lambda)$ of the acceptor:

$$J = \frac{\int F_D(\lambda)\varepsilon_A(\lambda)\lambda^4 d\lambda}{\int F_D(\lambda) d\lambda} \quad (3)$$

where λ is wavelength. The distance R between the donor and the acceptor in TnC-ME was calculated from the following equation:

$$E = R_0^6/(R_0^6 + R^6) \quad (4)$$

The orientation factor κ^2 cannot be determined uniquely. It is 2/3 if both emission and absorption dipoles rotate randomly over all orientations and are rapidly compared with the time-scale of energy transfer (dynamic averaging). This condition is not always met. Equations that gave the lower and upper bounds of κ^2 from steady-state polarization data were derived by Dale *et al.* (*42*):

```
                    1---5 ----10----15----20----25
ME Native :  NH3+-GIGAV,LKVLT,TGLPA,LISWI,KRKRQ,Q-CONH2
I2W/W19L  :  NH3+-G-GAV,LKVLT,TGLPA,LIS I,KRKRQ,Q-CONH2
V5W/W19L  :  NH3+-GIGA-,LKVLT,TGLPA,LIS I,KRKRQ,Q-CONH2
V8W/W19L  :  NH3+-GIGAV,LK-LT,TGLPA,LIS I,KRKRQ,Q-CONH2
L13W/W19L :  NH3+-GIGAV,LKVLT,TG-PA,LIS I,KRKRQ,Q-CONH2
```

Fig. 1. **Amino acid sequences of synthesized melittin derivatives, I2W/W19L, V5W/W19L, V8W/W19L, and L13W/W19L.** The altered amino acid residues are shown in outline.

$$\langle\kappa^2\rangle_{min}=(2/3)[1-(\langle d^x{}_D\rangle+\langle d^x{}_A\rangle)/2] \quad (5)$$

$$\langle\kappa^2\rangle_{max}=(2/3)[1+\langle d^x{}_D\rangle+\langle d^x{}_A\rangle+3\langle d^x{}_D\rangle\langle d^x{}_A\rangle] \quad (6)$$

where $\langle d^x{}_D\rangle$ and $\langle d^x{}_A\rangle$ are the axial depolarization factors of attached donor and acceptor, respectively. They are given by:

$$\langle d^x{}_D\rangle=(A_{0D}/A_{fD})^{1/2} \quad (7)$$

$$\langle d^x{}_A\rangle=(A_{0A}/A_{fA})^{1/2} \quad (8)$$

where A_{0D} and A_{0A} are the limiting anisotropies of the attached donor and attached acceptor, respectively, and A_{fD} and A_{fA} are the fundamental anisotropies of free donor and acceptor, respectively. The limiting anisotropies were determined experimentally for each chromophore under each set of conditions by extrapolating steady-state isothermal polarization data to infinite viscosity using glycerol (*43*). An ideal value of 0.4 was assumed for the fundamental anisotropy (*42*).

Each fluorescence energy transfer experiment was performed at 25.0±0.1°C in a medium containing 0.1 M KCl, 20 mM Tris-HCl, pH 7.5, and one of the following additions: (i) 4 mM EGTA, (ii) 4 mM $MgCl_2$ and 4 mM EGTA, or (iii) 5 mM $CaCl_2$ and 4 mM EGTA. These solutions are called EGTA, Mg^{2+}, Ca^{2+} solutions, respectively.

RESULTS AND DISCUSSION

The absorption spectra of TnC^{DANZ} and TnC^{AEDANS} and the fluorescence emission spectrum of TnC-ME are shown in Fig. 2. To exclude the fluorescence from the tyrosine residue in the TnC molecules, we adopted an excitation wavelength of 300 nm. These curves reveal the spectral overlap of donor (tryptophan in ME) emission and acceptor absorption. Figure 2 shows that DANZ and AEDANS are good acceptors of excitation energy from tryptophan. The quenching of the donor emission resulting from introduction of a DANZ acceptor or an AEDANS acceptor into the TnC-ME is depicted in Fig. 3. In contrast with TnC-ME TnC^{DANZ}-ME emits in two regions of the spectrum upon excitation at 300 nm. One is corresponds to the emission of the Trp residue of ME, and other to the emission of DANZ. The same tendency is observed in TnC^{AEDANS}-ME system. Values of F_D and F_{DA} were obtained by integrating the corrected fluorescence intensity between 300 and 400 nm for TnC^{DANZ}-ME, and between 300 and 370 nm for TnC^{AEDANS}-ME. In these wavelength regions, the fluorescence of the acceptor was negligible.

The fluorescence energy transfer efficiency from tryptophan of ME or its derivatives to DANZ or AEDANS of TnC and the donor-acceptor distance were evaluated and listed in Table I. The various spectroscopic parameters that were required to calculate the donor-acceptor distance are also listed in Table I.

In the following discussion, we consider the donor-acceptor distance based on the isotropic and random orientation of the donor and acceptor dipoles ($\kappa^2=2/3$). In the TnC^{DANZ}-ME system, the acceptor DANZ binds to Met-25 of helix A in the N-terminal domain of TnC. Donor-acceptor distance of this system is shown in Fig. 4 as a function

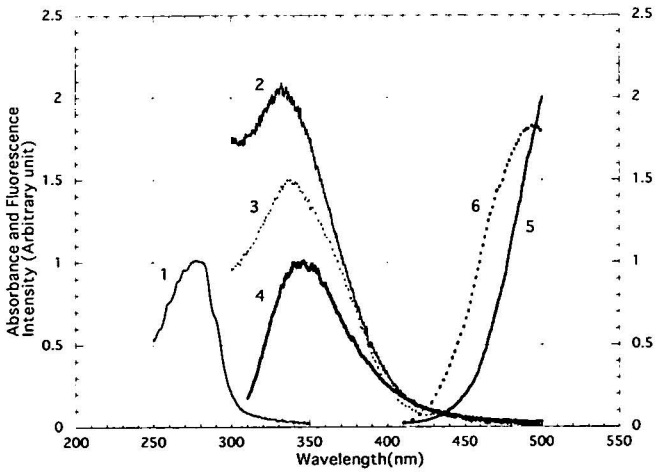

Fig. 2. **Fluorescence and absorption spectra of TnC-ME, TnC^{DANZ}, and TnC^{AEDANS}.** Curve 1, absorption spectrum of TnC-ME; curve 2, absorption spectrum of TnC^{DANZ}; curve 3, absorption spectrum of TnC^{AEDANS}; curve 4, fluorescence spectrum of TnC-ME; curve 5, fluorescence spectrum of TnC^{DANZ}; curve 6, fluorescence spectrum of TnC^{AEDANS}. Excitation wavelength was 300 nm for TnC-ME, 340 nm for TnC^{DANZ}, and 337 nm for TnC^{AEDANS}. Each curve was measured at 25°C in EGTA solution.

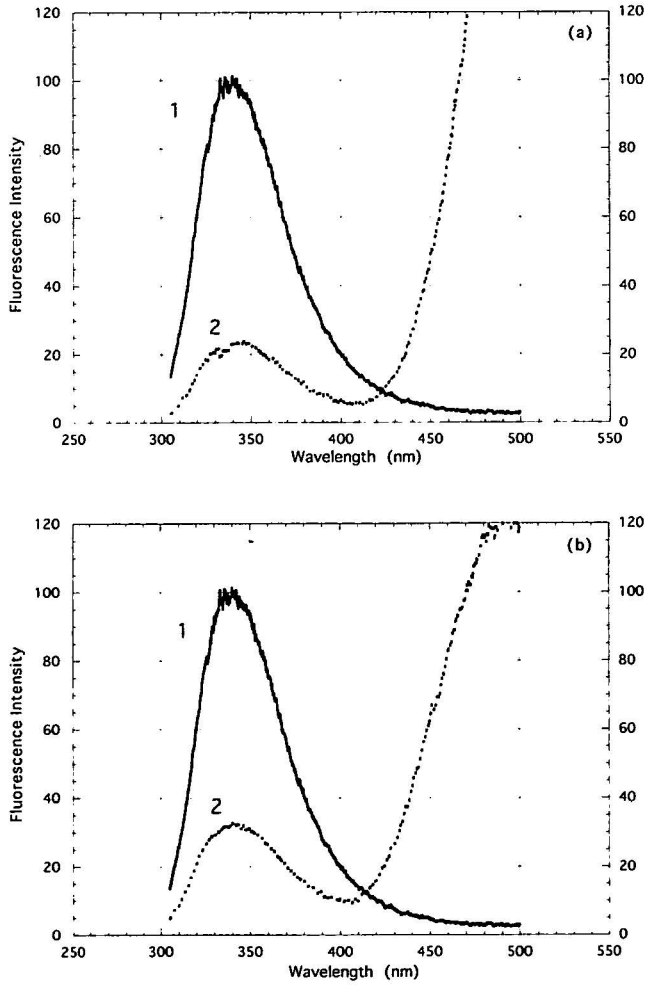

Fig. 3. **Fluorescence spectra of TnC-ME, TnC^{DANZ}-ME, and TnC^{AEDANS}-ME.** (a) TnC-ME (curve 1) and TnC^{DANZ}-ME (curve 2) in EGTA solution; (b) TnC-ME (curve 1) and TnC^{AEDANS}-ME (curve 2) in EGTA solution. TnC concentration was 5 μM. Excitation wavelength was 300 nm.

TABLE I-a. **Experimental fluorescence energy transfer data of TnC^{DANZ}-ME systems.**

	TnC-I2W/W19L			TnC-V5W/W19L			TnC-V8W/W19L			TnC-L13W/W19L			TnC-ME		
	EGTA	Mg^{2+}	Ca^{2+}	EGTA	Mg^{2+}	Ca^{2+}	EGTA	Mg^{2+}	Ca^{2+}	EGTA	Mg^{2+}	Ca^{2+}	EGTA	Mg^{2+}	Ca^{2+}
E (%)	72.8	54.7	55.9	73.5	40.7	55.8	66.2	52.4	50.8	67.0	48.4	67.4	87.5	82.7	95.5
J ($\times 10^9$ $M^{-1}\cdot cm^3$)	2.51	2.51	2.58	2.57	2.53	2.64	2.34	2.38	2.37	2.37	2.40	2.63	2.53	2.53	2.64
Q_d ($\times 10^{-2}$)	6.44	3.78	4.01	5.44	3.40	3.79	3.58	3.43	2.55	3.33	3.05	3.68	7.33	7.39	9.16
κ^2_{min} ($\times 10^{-2}$)	9.26	25.9	12.8	18.7	25.7	12.7	14.6	26.2	16.0	16.6	24.1	10.5	7.67	11.5	14.1
κ^2_{max}	3.27	2.20	3.02	2.63	2.24	3.05	2.89	2.21	2.77	2.78	2.33	3.17	3.39	3.14	2.96
$R_{0(2/3)}$ (Å)	18.5	16.9	17.2	18.1	16.6	17.1	16.6	16.5	15.7	16.4	16.2	17.0	18.9	19.0	19.8
$R_{0(min)}$ (Å)	13.3	14.4	13.1	14.7	14.2	13.0	12.9	14.1	12.4	13.0	13.7	12.5	13.2	14.2	15.3
$R_{0(max)}$ (Å)	24.1	20.6	22.1	22.8	20.3	22.0	21.2	20.2	19.9	20.8	20.0	22.0	24.8	24.6	25.4
$R_{(2/3)}$ (Å)	15.7	16.4	16.5	15.2	17.7	16.4	14.8	16.2	15.6	14.6	16.4	15.0	13.7	14.6	11.9
$R_{(min)}$ (Å)	11.3	14.0	12.5	12.3	15.1	12.4	11.5	13.9	12.3	11.6	13.8	11.0	9.55	10.9	9.18
$R_{(max)}$ (Å)	20.5	20.0	21.2	19.1	21.7	21.1	18.9	19.8	19.8	18.5	20.2	19.5	18.0	18.9	15.3

TABLE I-b. **Experimental fluorescence energy transfer data of TnC^{AEDANS}-ME systems.**

	TnC-I2W/W19L			TnC-V5W/W19L			TnC-V8W/W19L			TnC-L13W/W19L			TnC-ME		
	EGTA	Mg^{2+}	Ca^{2+}	EGTA	Mg^{2+}	Ca^{2+}	EGTA	Mg^{2+}	Ca^{2+}	EGTA	Mg^{2+}	Ca^{2+}	EGTA	Mg^{2+}	Ca^{2+}
E (%)	71.5	64.2	72.7	70.2	38.7	64.6	48.6	53.0	—[a]	77.7	73.6	98.8	90.6	92.3	—[a]
J ($\times 10^9$ $M^{-1}\cdot cm^3$)	2.48	1.67	1.93	2.51	1.64	1.94	2.35	1.58	1.84	2.40	1.62	1.97	2.52	1.69	2.01
Q_d ($\times 10^{-2}$)	6.44	3.78	4.01	5.44	3.40	3.79	3.58	3.43	2.55	3.33	3.05	3.68	7.33	7.39	9.16
κ^2_{min} ($\times 10^{-2}$)	9.30	29.6	11.0	25.3	24.4	14.9	25.0	21.5	22.1	24.2	21.4	13.3	10.7	17.1	11.2
κ^2_{max}	3.26	2.02	3.12	2.27	2.31	2.91	2.28	2.48	2.44	2.32	2.49	2.99	3.19	2.73	3.16
$R_{0(2/3)}$ (Å)	23.9	20.5	21.2	23.3	20.1	21.0	21.5	20.0	19.5	21.3	19.7	21.0	24.5	23.0	24.5
$R_{0(min)}$ (Å)	17.2	17.9	15.7	19.8	17.0	16.4	18.3	16.6	16.2	18.0	16.3	16.1	18.1	18.3	18.2
$R_{0(max)}$ (Å)	31.1	24.7	27.4	28.6	24.7	26.8	26.4	24.9	24.2	26.2	24.5	27.0	31.8	29.1	31.7
$R_{(2/3)}$ (Å)	20.5	18.6	18.0	20.2	21.7	19.0	21.7	19.6	—[b]	17.3	16.6	10.4	16.8	15.2	—[b]
$R_{(min)}$ (Å)	14.8	16.2	13.3	17.2	18.3	14.8	18.4	16.2	—	14.6	13.7	7.95	12.4	12.1	—
$R_{(max)}$ (Å)	26.7	22.4	23.3	24.8	26.7	24.3	26.6	24.4	—	21.3	20.7	13.4	21.8	19.2	—

[a]Donor fluoresence was completely quenched. [b]$R_{(2/3)}$ was lower than 8 Å.

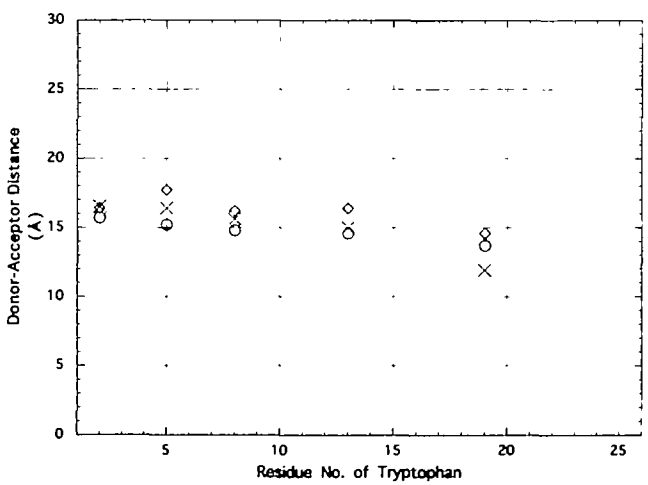

Fig. 4. **Distance between tryptophan of melittin and DANZ bound to Met-25 as a function of the position number of tryptophan of melittin.** Data were obtained in EGTA solution (○), Mg^{2+} solution (◇), and Ca^{2+} solution (×).

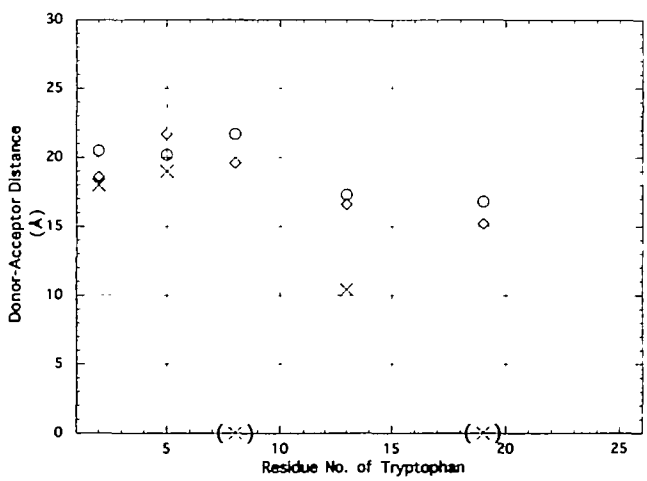

Fig. 5. **Distance between tryptophan of melittin and AEDANS bound to Cys-98 as a function of the position number of tryptophan of melittin.** Data were obtained in EGTA solution (○), Mg^{2+} solution (◇), and Ca^{2+} solution (×). Donor-acceptor distances of TnC^{AEDANS}-ME V8W and TnC^{AEDANS}-ME are much less than 8 Å.

of the position number of the Trp residue in ME and ME derivatives. Although the fluorescence energy transfer efficiency depended on the divalent cation-binding of TnC, the $R_{(2/3)}$ value did not remarkably depend on Mg^{2+}- and Ca^{2+}-binding of TnC. ($R_{(2/3)}$ is a donor-acceptor distance calculated under the assumption that $\kappa^2=2/3$.) In all solvent systems, the $R_{(2/3)}$ value was in the range of 11.9-17.7 Å, and their averaged value was 15.4 Å. This is because the divalent cation-dependent change of R_0 value cancels the divalent cation-dependent change of the fluorescence energy transfer efficiency. The other remarkable point of Fig. 4 is that the $R_{(2/3)}$ value does not depend on the position of the donor in ME derivatives. Melittin helix assumes the shape of a bent rod, with the bend at residues 11 and 12 and a bend angle of about 120 degree (*44*). Pro-14 contributes to the formation of the bend in the ME helix (*44*). Since all ME derivatives have Pro-14, it is reasonable to assume that ME derivatives bound to TnC take the bent rod structure of the ME molecule. All Trp residues of ME

and ME derivatives are on the "inner" side of the ME bent rod. Therefore there must be a position or positions of the acceptor for which the donor-acceptor distance does not remarkably depend on the position of the donor in the ME molecule.

In the case of TnC^{AEDANS}-ME, the acceptor binds to Cys-98 of helix E in the C-terminal domain of TnC. Figure 5 shows that the $R_{(2/3)}$ value of this system did not depend on the binding of Mg^{2+} to TnC. The $R_{(2/3)}$ value was in the range of 16.8-21.7 Å in EGTA solution and 15.2-21.7 Å in Mg^{2+} solution. The $R_{(2/3)}$ values of TnC^{AEDANS}-L13W/W19L and TnC^{AEDANS}-ME were smaller than the others. In Ca^{2+} solution, 100% energy transfer was observed in TnC^{AEDANS}-V8W/W19L and TnC^{AEDANS}-ME systems. The $R_{(2/3)}$ values of these systems were much smaller than 8 Å. The $R_{(2/3)}$ value of TnC^{AEDANS}-L13W/W19L was also very small (10.4 Å). Therefore, we conclude that, in Ca^{2+} solution, Trp residues in the central region of ME derivatives were close to Cys-98 of TnC. The distance between them was less than 10.4 Å.

Let us consider the relative position of Met-25 and Cys-98 of TnC and Trp-13 of L13W/W19L. In the presence of Ca^{2+}, we reported that $R_{(2/3)}$ between Met-25 and Cys-98 of TnC-ME complex was 50.0 Å (*28*). $R_{(2/3)}$ between Cys-98 of TnC and Trp-13 of L13W/W19L was determined in this work as 10.4 Å, and $R_{(2/3)}$ between Met-25 and Trp-13 as 15.0 Å. There is thus a discrepancy between our previous result and the present one. However, if we take $R_{(min)}$ of the previous report and $R_{(max)}$ of the present work, we can draw a picture of the relative positions of Met-25 and Cys-98 of TnC and Trp-13 of the ME derivative as follows. The maximum distance from Met-25 of TnC to Trp residue of ME derivatives is 19.5 Å (Table I), and the minimum distance from Met-25 to Cys-98 of TnC is 29.1 Å (*28*). If we estimate the distance from the Trp residue of the central region of ME derivatives to Cys-98 of TnC as 10 Å, the central region of ME must be located on the line connecting Met-25 and Cys-98. Met-25 is located near helix D and Cys-98 on helix E. Helix E, eleven linker residues, and helix D form a 31-residue central helix of TnC. Then the central region of ME is near to the C-terminal side of the central helix of TnC in Ca^{2+} solution.

In EGTA and Mg^{2+} solutions, donor-acceptor distance did not depend remarkably on the position of the Trp residue (Figs. 4 and 5). This suggests that the ME molecule is enfolded by the N- and C-terminal domains of TnC, and the ME rod is almost perpendicular to a line connecting Met-25 and Cys-98 of TnC. Since $R_{(2/3)}$ between DANZ and Trp is smaller than that between AEDANS and Trp (Table I), ME is located relatively near to the N-terminal domain of TnC in the absence of Ca^{2+}. The central region of ME is close to Cys-98 in the presence of Ca^{2+}, but moves away from Cys-98 in the absence of Ca^{2+}.

The axial depolarization factor gives information on the

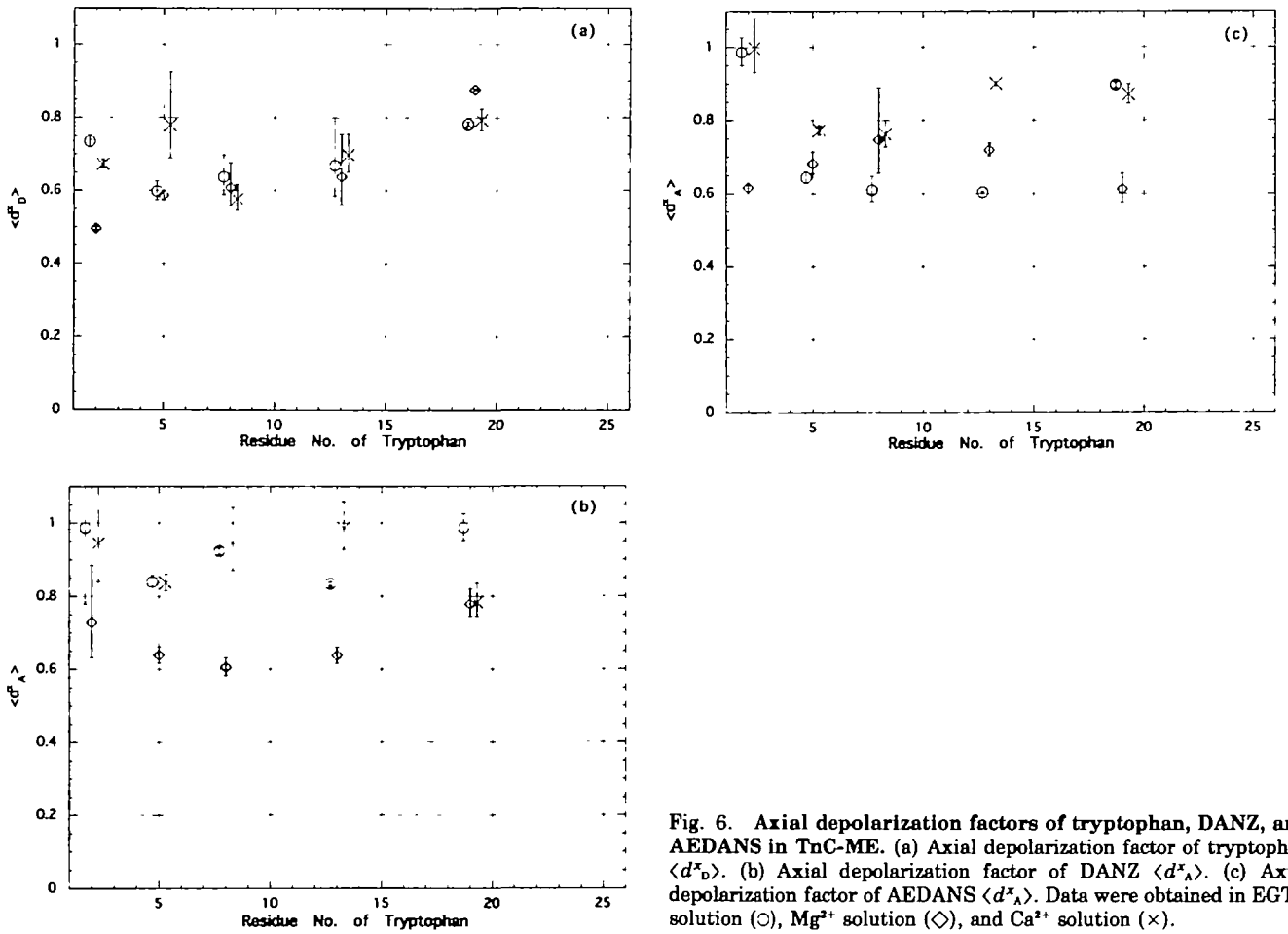

Fig. 6. Axial depolarization factors of tryptophan, DANZ, and AEDANS in TnC-ME. (a) Axial depolarization factor of tryptophan $\langle d^x_D \rangle$. (b) Axial depolarization factor of DANZ $\langle d^x_A \rangle$. (c) Axial depolarization factor of AEDANS $\langle d^x_A \rangle$. Data were obtained in EGTA solution (○), Mg^{2+} solution (◇), and Ca^{2+} solution (×).

rotation of the emission dipole of the chromophore. In this experiment, the values of $\langle d^x_D \rangle$ and $\langle d^x_A \rangle$ were calculated from A_{0D} and A_{0A}, which were determined from Perrin plots, and $A_{fD} = A_{fA} = 0.4$. Figure 6a shows that $\langle d^x_D \rangle$ of Trp-19 of ME is higher than the others. This means that random rotation of the emission dipole of Trp-19 is reduced as compared with the other Trp residues. Figure 6b reveals that DANZ bound to Met-25 of TnC shows lower $\langle d^x_A \rangle$ value in Mg^{2+} solution than in the other solutions. Donor-acceptor distance between DANZ and Trp is larger in Mg^{2+} solution than in the other solutions (Fig. 4). So the DANZ chromophore should rotate more freely in Mg^{2+} solution than in the other solutions. In EGTA and Ca^{2+} solutions, on the contrary, DANZ shows a high $\langle d^x_A \rangle$ value. This means that DANZ rotation is suppressed in the EGTA and Ca^{2+} solutions. Figure 6c shows the averaged value of $\langle d^x_A \rangle$ of AEDANS bound to Cys-98 is higher in Ca^{2+} solution (0.861) than in EGTA solution (0.748) and Mg^{2+} solution (0.675). The rotation of AEDANS chromophore is more suppressed in Ca^{2+} solution than in the other solutions. Figure 6c also reveals that AEDANS rotation is suppressed when ME has a Trp-2 or Trp-19 residue in Ca^{2+} and EGTA solutions. On the contrary, in Mg^{2+} solution, it gains rotational freedom when ME has Trp-2 or Trp-19. These results suggest an interaction between the Trp residue of ME and Cys-98 of TnC.

In this work, we used ME derivatives in which residue 2, 5, 8, or 13 of ME was replaced with a Trp residue. These residues, together with Trp-19, are on the inner side of the bent rod of ME (*44*). We can propose the whole three-dimensional structure of TnC-ME complex based on the donor-acceptor distances obtained in this work, donor-acceptor distance between DANZ and 5-(iodoacetamide) eosin bound to Met-25 and Cys-98 of TnC, respectively (*28*), and position coordinates of residues 2, 5, 8, 13, and 19 of ME (*45*). In both EGTA and Mg^{2+} solutions, ME binds to TnC in such a way that the outer side of the bent rod of ME faces the N-terminal side of the central helix of TnC and the residues 2, 5, 8, 13, and 19 of ME face down to the C-terminal domain of TnC. On the contrary, in Ca^{2+} solution, the outer side of the bent rod faces the C-terminal side of the central helix of TnC and the inner side of the bent rod faces up to the N-terminal domain of TnC. This change of ME position upon binding of Ca^{2+} to TnC may be a cause of the increase in distance between Met-25 and Cys-98 which accompanies the Ca^{2+}-binding, as was reported in the previous paper (*28*). The position of ME may also differ in EGTA solution and Mg^{2+} solution, as suggested by the data of $\langle d^x_A \rangle$ (Fig. 6b). The rotational freedom of DANZ bound to Met-25 of TnC is higher in Mg^{2+} solution than in EGTA solution. This suggests that ME is located father away from Met-25 in Mg^{2+} solution than in the EGTA solution.

The structure of TnC-ME complex in the Ca^{2+} solution described here resembles the computer-simulated model of Strynadka and James (*46*) except in one point: the inner side of the bent rod of ME faces the center of the C-terminal lobe of TnC in their model, while the outer side of the bent rod faces helix D of TnC in our model. Kobayashi *et al.* (*47*) reported that inhibitory peptide 104-115 of troponin I binds to two regions of TnC, residues 84-94 and 60-61, in the presence of Ca^{2+}. We revealed in this work that ME binds to both the N- and C-domains of TnC.

Calmodulin is a close homolog of TnC and has the same type of the crystal structure as TnC (*12*). Four-Ca^{2+}-bound calmodulin binds target proteins and activates them Ca^{2+}-dependently (*48*). Calmodulin also binds extracellular peptides such as melittin and mastoparan (*48*). Persechini and Kretsinger (*49*) proposed that the linker region of the central helix of calmodulin functions as a flexible tether permitting the two lobes to enfold an α-helix of the target protein, thereby activating Ca^{2+}-dependently the target protein. Ikura *et al.* (*21*) and Meador *et al.* (*50, 51*) have confirmed the proposal of Persechini and Kretsinger by multidimensional NMR spectroscopy and X-ray crystallography. Considering the close homology between TnC and calmodulin, it is reasonable to assume that the TnC-ME complex takes the same structure as the complex of calmodulin and its target peptide. Blechner *et al.* (*52*) reported small-angle X-ray scattering studies of TnC and TnC-ME systems. They revealed that Ca^{2+}-saturated TnC-ME assumed a significantly contracted globular structure. Their result and our data obtained here confirm the above proposal for the TnC-ME system. Furthermore, our data suggest that the TnC-ME system assumes the contracted globular structure even in the absence of Ca^{2+}.

REFERENCES

1. Ebashi, S. (1974) Regulatory mechanism of muscle contraction with special reference to the Ca-troponin-tropomyosin system. *Essays Biochem.* **10**, 1-36
2. Ebashi, S. and Endo, M. (1968) Calcium ion and muscle contraction. *Prog. Biophys. Mol. Biol.* **18**, 123-183
3. Ebashi, S. (1980) Regulation of muscle contraction. *Proc. R. Soc. London Ser. B* **207**, 259-286
4. Leavis, P.C. and Gergely, J. (1984) Thin filament proteins and thin filament-linked regulation of vertebrate muscle contraction. *CRC Crit. Rev. Biochem.* **16**, 235-305
5. Hertzberg, O. and James, M.N.G. (1985) Structure of the calcium regulatory muscle protein troponin-C at 2.8 Å resolution. *Nature* **313**, 653-659
6. Satyshur, K.A., Rao, S.T., Pyzalska, D., Drendel, W., Greaser, M., and Sundaralingam, M. (1988) Refined structure of chicken skeletal muscle troponin C in the two-calcium state at 2-Å resolution. *J. Biol. Chem.* **263**, 1628-1647
7. Potter, J.D. and Gergely, J. (1975) The calcium and magnesium binding site on tropnin and their role in the regulation of myofibrillar adenosine triphosphatase. *J. Biol. Chem.* **250**, 4628-4633
8. Collins, J.H., Greaser, M.L., Potter, J.D., and Horn, M.J. (1977) Determination of the amino acid sequence of troponin C from rabbit skeletal muscle. *J. Biol. Chem.* **252**, 6356-6362
9. Sin, I.L., Fernandes, R., and Mercola, D. (1978) Direct identification of the high and low affinity calcium binding sites of troponin C. *Biochem. Biophys. Res. Commun.* **82**, 1132-1139
10. Leavis, P.C., Rosenfeld, S.S., Gergely, J., Grabarek, Z., and Drabikowski, W. (1978) Proteolytic fragments of troponin C. Localization of high and low affinity Ca^{2+} binding sites and interactions with troponin I and troponin T. *J. Biol. Chem.* **253**, 5452-5459
11. Watterson, D.M., Sharief, F., and Vanaman, T.C. (1980) The complete amino acid sequence of the Ca^{2+}-dependent modulator protein (calmodulin) of bovine brain. *J. Biol. Chem.* **255**, 962-975
12. Babu, Y.S., Sack, J.S., Greenhough, T.J., Bugg, C.E., Means, A.R., and Cook, W.J. (1985) Three-dimensional structure of calmodulin. *Nature* **315**, 37-40
13. Grabarek, Z., Tao, T., and Gergely, J. (1992) Molecular mechanism of troponin-C function. *J. Muscle Res. Cell Motil.* **13**, 383-393
14. Herzberg, O., Moult, J., and James, M.N.G. (1986) A model for

the Ca^{2+}-induced conformational transition of troponin C. A trigger for muscle contraction. *J. Biol. Chem.* **261**, 2638-2644
15. Houdusse, A., Love, M.L., Dominguez, R., Grabarek, Z., and Cohen, C. (1997) Structures of four Ca^{2+}-bound troponin C at 2.0 Å resolution: further insights into the Ca^{2+}-switch in the calmodulin superfamily. *Structure* **5**, 1695-1711
16. Grabarek, Z., Tan, R.Y., Wang, J., Tao, T., and Gergely, J. (1990) Inhibition of mutant troponin C activity by an intradomain disulphide bond. *Nature* **345**, 182-184
17. Fujimori, K., Sorenson, M., Hertzberg, O., Moult, J., and Reinach, F.C. (1990) Probing the calcium-induced conformational transition of troponin C with site-directed mutants. *Nature* **345**, 182-184
18. Sellinger-Barnette, M. and Weiss, B. (1984) Interaction of various peptides with calmodulin. *Adv. Cyclic Nucleotide Protein Phosphorylation Res.* **16**, 261-276
19. DeGrado, W.F. (1988) Design of peptides and proteins. *Adv. Protein Chem.* **39**, 51-124
20. Habermann, V.E. and Jentsch, J. (1967) Sequenzanalyse des Melittins aus den tryptischen und peptischen Spaltstücken. *Hoppe-Seyler's Z. Physiol. Chem.* **348**, 37-50
21. Ikura, M., Clore, G.M., Gronenborn, A.M., Zhu, G., Klee, C.B., and Bax, A. (1992) Solution structure of a calmodulin-target peptide complex by multidimensional NMR. *Science* **256**, 632-638
22. Sheng, Z., Pan, B.S., Miller, T.E., and Potter, J.D. (1992) Isolation, expression, and mutation of a rabbit skeletal muscle cDNA clone for troponin I. The role of the NH_2 terminus of fast skeletal muscle troponin I in its biological activity. *J. Biol. Chem.* **267**, 25407-25413
23. Tablot, J.A. and Hodges, R.S. (1981) Synthetic studies on the inhibitory region of rabbit skeletal troponin I. Relationship of amino acid sequence to biological activity. *J. Biol. Chem.* **256**, 2798-2802
24. Dalgarno, D.C., Grand, R.J.A., Levine, B.A., Moir, A.J.G., Scott, G.M.M., and Perry, S.V. (1982) Interaction between troponin I and troponin C. Definition of the topography by proton magnetic resonance spectroscopy. *FEBS Lett.* **150**, 54-58
25. Cachia, P.J., Sykes, B.D., and Hodges, R.S. (1983) Calcium-dependent inhibitory region of troponin: A proton nuclear magnetic resonance study on the interaction between troponin C and the synthetic peptide N^{α}-acetyl[$FPhe^{106}$]TnI-(104-115) amide. *Biochemistry* **22**, 4145-4152
26. van Eyk, J. and Hodges, R.S. (1988) The biological importance of each amino acid residue of the troponin I inhibitory sequence 104-115 in the interaction with troponin C and tropomyosin-actin. *J. Biol. Chem.* **263**, 1726-1732
27. Wang, C.K. and Cheung, H.C. (1986) Proximity relationship in the binary complex formed between troponin I and troponin C. *J. Mol. Biol.* **190**, 509-521
28. Sano, H. and Iio, T. (1995) Fluorescence energy transfer study of troponin C-melittin complex. *J. Biochem.* **118**, 996-1000
29. Ebashi, S., Kodama, A., and Ebashi, F. (1968) Troponin I. Preparation and physiological function. *J. Biochem.* **64**, 465-477
30. van Eerd, J.P. and Kawasaki, Y. (1973) Effect of calcium(II) on the interaction between the subunits of troponin and tropomyosin. *Biochemistry* **12**, 4972-4980
31. Murray, A.C. and Kay, C.M. (1972) Hydrodynamic and optical properties of troponin A. Demonstration of a conformational change upon binding calcium ion. *Biochemistry* **11**, 2622-2627
32. Maulet, Y., Prevot, B.M., Kaiser, G., Rüegg, U.T., and Fulpius, B.W. (1980) Purification and chemical characterization of melittin and acetylated derivatives. *Biochim. Biophys. Acta* **625**, 274-280
33. Maulet, Y. and Cox, J.A. (1983) Structural changes in melittin and calmodulin upon complex formation and their modulation by calcium. *Biochemistry* **22**, 5680-5686
34. Johnson, J.D., Collins, J.H., and Potter, J.D. (1978) Dansylaziridine-labeled troponin C. A fluorescent probe of Ca^{2+} binding to the Ca^{2+}-specific regulatory sites. *J. Biol. Chem.* **253**, 6451-6458
35. Grabarek, Z., Grabarek, J., Leavis, P.C., and Gergely, J. (1983) Cooperative binding to the Ca^{2+}-specific sites of troponin C in regulated actin and actomyosin. *J. Biol. Chem.* **258**, 14098-14102
36. Hudson, E.N. and Weber, G. (1973) Synthesis and characterization of two fluorescent sulfhydryl reagents. *Biochemistry* **21**, 4154-4161
37. Lowry, O.H., Rosebrough, N.J., Farr, A.L., and Randall, R.J. (1951) Protein measurement with the folin phenol reagent. *J. Biol. Chem.* **193**, 265-275
38. Stryer, L. (1978) Fluorescence energy transfer as a spectroscopic ruler. *Annu. Rev. Biochem.* **47**, 819-846
39. Fairclough, R.H. and Cantor, C.R. (1978) The use of singlet-singlet energy transfer to study macromolecular assemblies. *Methods Enzymol.* **48**, 347-379
40. Förster, T. (1948) Zwischenmolekulare Energiewanderung und Fluoreszenz. *Ann. Physik* **6**, 55-75
41. Melhuish, W.H. (1961) Quantum efficiencies of fluorescence of organic substances: Effect of solvent and concentration of the fluorescent solute. *J. Phys. Chem.* **65**, 229-235
42. Dale, R.F., Eisinger, J., and Blumberg, W.E. (1979) The orientational freedom of molecular probes. The orientation factor in intramolecular energy transfer. *Biophys. J.* **26**, 161-194
43. Weber, G. (1953) Rotational Brownian motion and polarization of fluorescence of solutions. *Adv. Protein Chem.* **8**, 415-459
44. Terwilliger, T.C. and Eisenberg, D. (1981) The structure of melittin. II. Interpretation of the structure. *J. Biol. Chem.* **257**, 6016-6022
45. Terwilliger, T.C. and Eisenberg, D. (1981) The structure of melittin. I. Structure determination and partial refinement. *J. Biol. Chem.* **257**, 6010-6015
46. Strynadka, N.C.J. and James, M.N.G. (1990) Model for the interaction of amphiphilic helices with troponin C and calmodulin. *Proteins Struct. Funct. Genet.* **7**, 234-248
47. Kobayashi, T., Leavis, P.C., and Collins, J.H. (1996) Interaction of a troponin I inhibitory peptide with both domains of troponin C. *Biochim. Biophys. Acta* **1294**, 25-30
48. Crivici, A. and Ikura, M. (1995) Molecular and structural basis of target recognition by calmodulin. *Annu. Rev. Biophys. Biomol. Struct.* **24**, 85-116
49. Persechini, A. and Kretsinger, R.H. (1988) Toward a model of the calmodulin-myosin light-chain kinase complex: Implications for calmodulin function. *J. Cardiovasc. Pharmacol.* **12**, S1-S12
50. Meador, W.E., Means, A.R., and Quiocho, F.A. (1992) Target enzyme recognition by calmodulin: 2.4 Å structure of a calmodulin-peptide complex. *Science* **257**, 1251-1255
51. Meador, W.E., Means, A.R., and Quiocho, F.A. (1993) Modulation of calmodulin plasticity in molecular recognition on the basis of X-ray structures. *Science* **262**, 1718-1721
52. Blechner, S.L., Olah, G.A., Strynadka, N.C.J., Hodges, R.S., and Trewhella, J. (1992) $4Ca^{2+}$·troponin C forms dimers in solution at neutral pH that dissociate upon binding various peptides: Small-angle X-ray scattering studies of peptide-induced structural changes. *Biochemistry* **31**, 11326-11334